Mon. Not. R. Astron. Soc. **000**, 1–?? (2010) Printed 9 September 2014 (MN LATEX style file v2.2)

Evolution of linear warps in accretion discs and applications to protoplanetary discs in binaries

Francois Foucart[1⋆] and Dong Lai[2]
[1] *Canadian Institute for Theoretical Astrophysics, University of Toronto, Toronto, Ontario M5S 3H8, Canada*
[2] *Department of Astronomy, Cornell University, Ithaca, NY 14853, USA*

arXiv:1406.3331v2 [astro-ph.EP] 8 Sep 2014

9 September 2014

ABSTRACT

Warped accretion discs are expected in many protostellar binary systems. In this paper, we study the long-term evolution of disc warp and precession for discs with dimensionless thickness H/r larger than their viscosity parameter α, such that bending waves can propagate and dominate the warp evolution. For small warps, these discs undergo approximately rigid-body precession. We derive analytical expressions for the warp/twist profiles of the disc and the alignment timescale for a variety of models. Applying our results to circumbinary discs, we find that these discs align with the orbital plane of the binary on a timescale comparable to the global precession time of the disc, and typically much smaller than its viscous timescale. We discuss the implications of our finding for the observations of misaligned circumbinary discs (such as KH 15D) and circumbinary planetary systems (such as Kepler-413); these observed misalignments provide useful constraints on the uncertain aspects of the disc warp theory. On the other hand, we find that circumstellar discs can maintain large misalignments with respect to the plane of the binary companion over their entire lifetime. We estimate that inclination angles larger than $\sim 20^\circ$ can be maintained for typical disc parameters. Overall, our results suggest that while highly misaligned circumstellar discs in binaries are expected to be common, such misalignments should be rare for circumbinary discs. These expectations are consistent with current observations of protoplanetary discs and exoplanets in binaries, and can be tested with future observations.

Key words: accretion, accretion discs – hydrodynamics – planetary systems: protoplanetary discs – stars: binary

1 INTRODUCTION

Warped accretion discs are expected in a variety of astrophysical systems, such as protoplanetary discs, discs around spinning black holes, remnant discs following neutron star binary mergers and stellar tidal disruption by massive black holes. In particular, in proto-stellar binary systems, both circumstellar discs and circumbinary discs are likely formed with inclined orientations, as a consequence of the complex star/binary/disc formation processes (e.g., Bate et al. 2003; McKee & Ostriker 2007; Klessen 2011). Indeed, a number of binary young stellar objects (YSOs) are observed to contain circumstellar discs that are misaligned with the binary orbital plane (e.g., Stapelfeldt et al. 1998). Observations of jets along different directions in unresolved YSOs also suggest the existence of misaligned discs (e.g., Davis, Mundt & Eislöffel 1994; Roccatagliata et al. 2011). Additionally, imaging of circumbinary debris discs show that while the disc plane and the binary orbital plane are aligned for some systems (such as α CrB, β Tri and HD 98800), significant misalignments can occur in others (such as 99 Herculis, with mutual inclination $\gtrsim 30^\circ$; see Kennedy et al. 2012a,b). Finally, the pre-main sequence binary KH 15D is surrounded by a precessing circumbinary disc inclined with respect to the binary plane by 10°-20° (e.g., Winn et al. 2004; Chiang & Murray-Clay 2004; Capelo et al. 2012), while in the FS Tauri system, circumbinary and circumstellar discs appear to be misaligned (Hioki et al. 2011).

Also of relevance is the recent discovery of transiting planetary systems around stellar binaries (e.g., Doyle et al. 2011; Welsh et al. 2012; Orosz et al. 2012; Kostov et al. 2014). While most of these systems have the binary orbital plane and the planetary orbital plane consistent with alignment, a small misalignment ($\sim 2.5^\circ$) has been found in the Kepler-413 system (consisting of a Neptune-size planet orbiting an eclipsing stellar binary; Kostov et al. 2014).

⋆ Email: ffoucart@cita.utoronto.edu

A potential explanation for this misalignment is that the planet formed in a circumbinary disc misaligned with respect to its host binary. Understanding the inclination distribution of circumbinary planets is important for determining the abundance and the formation scenarios of these planets (e.g., Martin & Triaud 2014; Armstrong et al. 2014).

Theoretical studies of the evolution of misaligned accretion discs have been performed under the assumption of small warps in the discs, with numerical simulations providing information for the behavior of discs with larger warps. For discs in which the viscosity parameter α is smaller than H/r (with H the scaleheight of the disc), bending waves can propagate warps through the disc at about half the disc sound speed (Papaloizou & Lin 1995). This rapid communication allows a misaligned disc experiencing an external torque to precess approximately as a rigid body, as long as the precession timescale of the disc is longer that the time required for bending waves to travel across the disc (Papaloizou & Terquem 1995). This analytical prediction has been verified by 3D numerical simulations of circumstellar discs using both smoothed particle hydrodynamics (Larwood & Papaloizou 1997) and finite volume methods (Fragner & Nelson 2010). Smoothed particle simulations of narrow circumbinary discs have provided similar results (Facchini et al. 2013). Recent numerical simulations have also been used to explore the limitations of the linear theory (Fragner & Nelson 2010; Sorathia et al. 2013a).

A one-dimensional model for the evolution of small warps in a thick disc has been developed by Lubow & Ogilvie 2000 (see also Lubow et al. 2002, Ogilvie 2006), and used to study the evolution of circumstellar discs. In particular, Lubow & Ogilvie (2000) used this model to study misaligned circumstellar discs in binaries, and compute discrete eigenmodes of the warp. They found that, for specific values of the outer radius of the disc, unstable modes exist which can drive the growth of the disc inclination. Away from these resonant radii, the inclination of the disc is damped on a timescale which can be computed numerically by solving an eigenvalue problem. An analytical estimate for the damping rate of the inclination of circumstellar disc has also been proposed by Bate et al. (2000), based on a global estimate of the energy dissipation in the disc due to viscous torques. This damping timescale is generally of the order of the viscous timescale of the disc. However, Gammie et al. (2000) found that even when the disc warp is small enough to satisfy the linear theory, the disc may still be susceptible to parametric instabilities, whose effect on the long term evolution of the disc is currently uncertain. Bate et al. (2000) postulate that parametric instabilities will cause the damping of the inclination on a timescale comparable to the growth timescale of the instability, and would cause circumstellar discs to rapidly align within an angle of the order of the disc thickness H/r. Estimates of the condition under which parametric instabilities can grow, and of their growth rate have more recently been improved by the work of Ogilvie & Latter (2013),

Some of the results obtained for circumstellar discs can be applied to the less studied circumbinary discs. The condition and the timescale for global precession (Papaloizou & Terquem 1995) can be similarly obtained, and the approximate formula for the damping of the disc inclination proposed by Bate et al. (2000) appears to match the results of one-dimensional simulations performed by Facchini et al. (2013) to within factors of a few. The disc profile and the alignment of the disc-binary system were also studied in the limit of infinite circumbinary discs by Foucart & Lai (2013), and the evolution of finite size discs towards an equilibrium warped profile has been demonstrated numerically by Facchini et al. (2014).

In this paper, we study in more details the warp profile of both circumstellar and finite circumbinary discs. Building on the methods of Papaloizou & Terquem (1995) and on the eigenmode decomposition performed by Lubow & Ogilvie (2000), we provide approximate analytical expressions for the orientation profile of the disc and the damping timescale of the inclination by considering the properties of the lowest order-mode. With the warping profile closest to a flat disc, such a low-order mode has the smallest internal stresses and the longest lifetime, and will dominate the long term evolution of the disc. We show that these approximate formulae are correct to first order in the disc warp, and provide solutions which match well the results obtained both by solving the eigenvalue problem exactly, and by full 3D simulations. In particular, our results allow for the computation of the damping timescale of the disc inclination (both for circumstellar discs with an external binary companion and for circumbinary discs), which is much more accurate than the formula previously derived by Bate et al. (2000), without the need for expensive simulations or the explicit solution of an eigenvalue problem. Because we directly recover the orientation of the disc at all radii, we can also easily compare our disc warp profiles with the predictions of Ogilvie & Latter (2013) for the local conditions leading to the growth of parametric instabilities, and thus obtain improved estimates on the conditions under which these instabilities might affect the evolution of the disc. We show that circumstellar discs are likely to be able to maintain significant misalignments with respect to the orbital plane of a binary companion, in contrast to the early conclusion of Bate et al. (2000).

In Sec. 2 we present our analytical model for disc warps and inclination damping, and compare our results with numerical solutions. We then apply our calculations to the study of circumbinary discs in Sec. 3, and circumstellar discs in Sec. 4. We consider the effects of parametric instabilities in Sec. 5. In Sec. 6 we revisit the case of the KH 15D system, and examine how our results impact the interpretation of that system as a truncated circumbinary disc (Winn et al. 2004, Chiang & Murray-Clay 2004, Lodatto & Facchini 2013). In Sec. 7 we summarize our results and discuss their implications.

2 DISC WARP AND INCLINATION DAMPING: THEORETICAL MODEL AND ANALYTICAL SOLUTIONS

We consider the evolution of an accretion disc in the gravitational potential

$$\Phi(\mathbf{r}) = -\frac{GM}{r} + \delta\Phi(r,z), \tag{1}$$

assuming that the deviation $\delta\Phi$ from the pure Keplerian potential ($-GM/r$) is small (in a sense to be specified below). For circumbinary discs, we have $M = M_1 + M_2$ with $M_{1,2}$ the masses of the two binary components; for circumstellar

discs, we have $M = M_\star$ with $M_\star$ the mass of the central star. The potential $\delta\Phi(r,z)$ is axisymmetric, with the coordinate z along its symmetry axis, the angular momentum axis of the binary. We also assume that $\delta\Phi$ is either time-independent or time-averaged. The disc is generally misaligned with respect to the z-axis, with the angular momentum of the disc element at radius r lying at time t in the direction $\hat{\boldsymbol{l}}(r,t)$. In cartesian coordinates, we write

$$\hat{\boldsymbol{l}}(r,t) = (\sin\beta\cos\phi, \sin\beta\sin\phi, \cos\beta), \tag{2}$$

where $\beta(r,t)$ is the warp angle (the inclination of $\hat{\boldsymbol{l}}$ relative to the z-axis), and $\phi(r,t)$ is the twist angle (corresponding to the rotation of $\hat{\boldsymbol{l}}$ around the z-axis).

We consider a vertically integrated model for the disc, with surface density Σ and integrated pressure given by

$$\Sigma = \int \rho\, dz, \quad P = \int p\, dz = \Omega_z^2 \Sigma H^2. \tag{3}$$

Here ρ is the density in the disc, p the pressure, Ω_z the frequency for vertical oscillations in the potential Φ, and H is an effective scale height defined by Eq. (3). We also define $c_s = H\Omega_z$. For a vertically isothermal disc, c_s is the isothermal sound speed and H the usual Gaussian scale height (see Lubow et al. 2002). If the disc warp is linear, i.e., if the variation of the disc orientation satisfies $\psi \equiv |\partial\hat{\boldsymbol{l}}/\partial \ln r| \ll 1$, theoretical studies of α-discs (with isotropic viscosity $\nu = \alpha H^2 \Omega$, where α is the Shakura-Sunyaev parameter, and Ω is the angular velocity) have shown that the evolution of the warp follow two possible behaviors (Papaloizou & Pringle 1983; Papaloizou & Lin 1995). For discs with $H/r \lesssim \alpha$, the warp satisfies a diffusion-type equation with the diffusion coefficient $\nu_2 = \nu/(2\alpha^2)$, at least for $\alpha \ll 1$ (see Ogilvie 1999 and Lodato & Price 2010 for analytical and numerical studies of the effects of a larger α). For thicker discs ($H/r \gtrsim \alpha$), the warp propagates as bending waves at about half the sound speed c_s and dams on a timescale $1/(\alpha\Omega)$. In the latter case, the numerical simulations of Sorathia et al. (2013a) suggest that the linear theory remains valid for small warp satisfying $\psi \equiv |\partial\hat{\boldsymbol{l}}/\partial \ln r| \leqslant H/r$ while for stronger warps nonlinear effects cause rapid damping of the inclination of the disc. For larger viscosities, bending waves damp on a length scale shorter than the scale height of the disc, and do not propagate across the disc. In this paper, we will consider discs with $H/r \gtrsim \alpha$, which are relevant for a large class of astrophysical systems including protoplanetary discs.

For discs with $H/r \gtrsim \alpha$ and linear warps, the orientation of the disc evolves according to (Lubow & Ogilvie 2000; see also Lubow et al. 2002 and Ogilvie 2006)

$$\Sigma r^2 \Omega \frac{\partial \hat{\boldsymbol{l}}}{\partial t} = \frac{1}{r}\frac{\partial \boldsymbol{G}}{\partial r} + \Sigma r^2 \Omega^2 \left(\frac{\Omega^2 - \Omega_z^2}{2\Omega^2}\right) \hat{\mathbf{e}}_z \times \hat{\boldsymbol{l}}, \tag{4}$$

$$\frac{\partial \boldsymbol{G}}{\partial t} = \frac{\Sigma c_s^2 r^3 \Omega}{4}\frac{\partial \hat{\boldsymbol{l}}}{\partial r} + \left(\frac{\Omega^2 - \kappa^2}{2\Omega^2}\right) \Omega \hat{\mathbf{e}}_z \times \boldsymbol{G} - \alpha\Omega \boldsymbol{G}, \tag{5}$$

where $\hat{\mathbf{e}}_z$ is the unit vector along the z-axis, $\mathbf{G}$ is the internal stress in the disc, and Ω_z and κ are the vertical and radial epicyclic oscillation frequencies. The first term on the right-hand side of Eqs. (4)-(5) describe the free propagation of bending waves in the disc. The last term in Eq. (4) corresponds to the external torque that the potential $\delta\Phi$ applies on the misaligned disc. The last two terms in Eq. (5) arise from periastron advance for non-Keplerian orbits and from viscous damping in the disc, respectively. For small misalignments between $\hat{\boldsymbol{l}}$ and $\hat{\mathbf{e}}_z$, the frequencies Ω_z and κ can be computed according to

$$\kappa^2 = \frac{2\Omega}{r}\frac{d(r^2\Omega)}{dr}, \tag{6}$$

$$\Omega_z^2 = \left(\frac{\partial^2 \Phi}{\partial z^2}\right)_{z=0}. \tag{7}$$

The validity of Eqs. (4)-(5) requires a small deviation from the Keplerian potential, i.e., $|\kappa^2 - \Omega^2| \lesssim \delta\Omega^2$ and $|\Omega_z^2 - \Omega^2| \lesssim \delta\Omega^2$, where $\delta = H/r$. Under these assumptions, Eqs. (4-5) have been shown to reproduce the results of 3D numerical simulations for the evolution of linear warps (see, e.g., Larwood & Papaloizou 1997 for circumstellar discs, or Facchini et al. 2013 for circumbinary discs). For large misalignments between $\hat{\boldsymbol{l}}$ and $\hat{\mathbf{e}}_z$, Eqs. (6-7) would have to be corrected to appropriately reflect the time-averaged effects of the gravitational potential on the warp in a plane different from $z = 0$, but the general properties of the equations are left unchanged. This should be contrasted with the requirements of a quasi-Keplerian potential and of a small warp $|\partial\hat{\boldsymbol{l}}/\partial \ln r| \ll 1$, which are both necessary for the linear theory of bending wave propagation to apply.

There are however a couple of important caveats to keep in mind when using this one-dimensional model for the warp evolution. The first is that it was derived under the assumption of isotropic viscosity $\nu = \alpha H^2 \Omega$. In general, the viscosity may be anisotropic, and there is thus no guarantee that, in such case, the viscosity parameter α entering Eq. (5) is identical to the viscosity parameter responsible for the radial transfer of mass and angular momentum. Shearing box simulations of turbulence have found reasonable agreement with the assumption of isotropic viscosity (Torkelsson et al. 2000), at least as far as its influence on the damping parameter α is concerned. But recent global simulations find that the viscosity generated by the magnetorotational instability is anisotropic (Sorathia et al. 2013b, Teixeira et al. 2014). In practice, we can take α as a simplified parametrization of all the physical effects causing a damping of bending waves in the disc.

The second caveat is that, even in the linear regime, the disc warp may be unstable to a parametric instability and the development of turbulence due to the strong vertical shear in the flow velocity (Gammie et al. 2000; Ogilvie & Latter 2013). When this occurs, the behavior of the disc warp is uncertain. One reasonable proposal is that the damping of the disc warp would then be set by the growth rate of the instability (Bate et al. 2000). For a given disc profile, the parametric instability would then effectively set a minimum value for α. We discuss this issue in more detail in Sec. 5.

Despite these limitations, the linear model for the propagation of bending waves remains a useful tool to obtain approximate solutions to the evolution of warped discs, without having to resort to expensive numerical simulations that include all the microphysical effects required to recover the exact form of the viscosity in the disc. In the following, we derive analytical approximations for the main properties of the disc (warp amplitude, internal stress, global precession frequency, damping timescale of the warp) for configurations in which the disc, as a result of external torques, undergoes an approximately solid-body precession. We then compare these analytical results with numerical solutions in Sec. 2.4.

2.1 Warp equations as an eigenvalue problem

For time-independent (or time-averaged) potentials Φ, the solution of the evolution equations for $\hat{\boldsymbol{l}}$ and $\boldsymbol{G}$ can be written as a sum of eigenmodes

$$\hat{\boldsymbol{l}}(r,t) = \Re\left(\sum_\omega \tilde{\boldsymbol{l}}_\omega(r) e^{-i\omega t}\right), \tag{8}$$

$$\boldsymbol{G}(r,t) = \Re\left(\sum_\omega \tilde{\boldsymbol{G}}_\omega(r) e^{-i\omega t}\right), \tag{9}$$

where ω is the complex eigenfrequency of the mode, and $(\tilde{\boldsymbol{l}}_\omega, \tilde{\boldsymbol{G}}_\omega)$ are complex functions of the radius r. Physically, the real part of ω corresponds to the global precession of the angular momentum of the disc around the symmetry axis of the gravitational potential if $\tilde{\boldsymbol{l}}_{\omega,y} = \pm i\tilde{\boldsymbol{l}}_{\omega,x}$ (which, as we will see below, is always the case). Its imaginary part corresponds to the exponential damping of the warp (or exponential growth, if the mode is unstable). Global precession is possible as long as the small warp condition $|\partial\hat{\boldsymbol{l}}/\partial \ln r| \ll 1$ is satisfied. Papaloizou & Terquem (1995) showed that this is roughly equivalent to the condition

$$\Re(\omega) \lesssim \frac{H}{r}\Omega(r_{\rm out}), \tag{10}$$

which can be rephrased as the condition that the precession timescale is longer that the travel time of bending waves across the disc (as bending waves travel at half the sound speed $c_s \sim H\Omega$).

Each eigenmode then satisfies a set of four complex ODEs:

$$\frac{d\tilde{G}_x}{dr} = \Sigma r^3\Omega\left(-i\omega\tilde{l}_x + Z(r)\Omega\tilde{l}_y\right) \tag{11}$$

$$\frac{d\tilde{G}_y}{dr} = \Sigma r^3\Omega\left(-i\omega\tilde{l}_y - Z(r)\Omega\tilde{l}_x\right) \tag{12}$$

$$\frac{\Sigma c_s^2 r^3\Omega}{4}\frac{d\tilde{l}_x}{dr} = (-i\omega+\alpha\Omega)\tilde{G}_x + K(r)\Omega\tilde{G}_y \tag{13}$$

$$\frac{\Sigma c_s^2 r^3\Omega}{4}\frac{d\tilde{l}_y}{dr} = (-i\omega+\alpha\Omega)\tilde{G}_y - K(r)\Omega\tilde{G}_x, \tag{14}$$

where we have defined

$$K(r) = \frac{\Omega^2-\kappa^2}{2\Omega^2}, \tag{15}$$

$$Z(r) = \frac{\Omega^2-\Omega_z^2}{2\Omega^2}, \tag{16}$$

and dropped the subscripts ω for convenience. These equations can be solved as an eigenvalue problem once proper boundary conditions are chosen at the inner and outer edges of the disc. For the finite size discs considered in this paper, we will adopt the zero-torque boundary condition: $G(r_{\rm in}) = G(r_{\rm out}) = 0$.

The four ODEs (11)-(14) can easily be reduced to two sets of ODEs which are only coupled by sharing the same eigenfrequency ω. Defining $W_\pm = \tilde{l}_x \pm i\tilde{l}_y$ and $G_\pm = \tilde{G}_x \pm i\tilde{G}_y$, we find (see Lubow et al. 2002)

$$\frac{dG_\pm}{dr} = -i\Sigma r^3\Omega W_\pm(\omega \pm Z\Omega) \tag{17}$$

$$\frac{dW_\pm}{dr} = \frac{4G_\pm}{\Sigma r^3 c_s^2\Omega}(-i\omega+\alpha\Omega\mp iK\Omega). \tag{18}$$

In practice, the modes come in pairs (one with $W_+ = 0$, the other with $W_- = 0$), related by $W_+ = W_-^*$, $G_+ = G_-^*$ and $\omega_+ = -\omega_-^*$. The real part of $\tilde{\mathbf{l}}$ and $\tilde{\mathbf{G}}$ are the same for each mode in the pair, and the physical content of the two modes is thus identical. Accordingly, we only have to consider one set of modes. From now on, we will assume $\tilde{l}_y = i\tilde{l}_x$ (a pure W_- mode, with $W_+ = 0$).

Numerical solutions to a similar set of equations have already been obtained for circumstellar discs in binary systems (Lubow & Ogilvie 2000). Compared with circumbinary discs, which will be our main application here, an important difference is that for circumstellar discs the eigenmodes are a mixture of W_+ and W_-, because the driving of the disc at the orbital frequency Ω_b of the binary cannot always be neglected (Lubow & Ogilvie 2000 in fact solved the equations in a frame corotating with the binary), i.e. the assumption that the potential can be time-averaged breaks down. Lubow & Ogilvie (2000) showed that this additional effect is small for most disc parameters, but can cause resonances at specific locations in the the outer region of the disc, leading to a growing misalignment between the circumstellar disc and the binary.

In the following, we will focus on circumbinary discs, although the equations derived here are valid for any configuration in which the perturbing potential can be time-averaged – we will discuss the behavior of circumstellar discs away from resonances in Sec. 4. In Sec. 2.4 we present numerical solutions for the warp equations and the inclination damping rate. To gain more insight into the properties of the solutions for generic external potentials and disc profiles, however, it is useful to obtain analytical approximations to the numerical results. In the following subsections, we discuss such an approximate treatment for the lowest order warp mode of the disc – which in general has the slowest damping rate, and will thus dominate the long-term evolution of the warp (high-order modes are also more likely to violate the small warp condition, and are thus likely to damp even faster than predicted in the linear theory).

2.2 Approximate analytical solutions

To obtain an approximate solution for the lowest order eigenmode of the warp, we assume that this mode is a small correction to the flat disc configuration. It is also convenient to rotate the coordinates to a frame following the twist of the disc. Let the warp angle be $l_\theta(r) = \sin\beta(r)$ and the twist angle be $\phi(r)$, so that $l_x + il_y = l_\theta(r)\exp[i\phi(r)]$. Define the unit vectors

$$\hat{e}_\theta = \cos[\phi(r,t)]\hat{e}_x + \sin[\phi(r,t)]\hat{e}_y \tag{19}$$

$$\hat{e}_\phi = -\sin[\phi(r,t)]\hat{e}_x + \cos[\phi(r,t)]\hat{e}_y. \tag{20}$$

We consider a mode with $\tilde{l}_y = i\tilde{l}_x$ and $\tilde{G}_y = i\tilde{G}_x$, and solve for the disc profile at $t = 0$ (i.e. the real part of $\tilde{l}, \tilde{G}$). We also define

$$\omega = \omega_p - i\gamma, \tag{21}$$

with ω_p the precession rate of the disc, and γ the damping rate of the disc inclination. In that frame, $l_\phi = 0$ (by the definition of $\hat{e}_\phi$) and the eigenmode satisfies the following

(real) equations

$$\frac{dG_\phi}{dr} = \Sigma r^3\Omega[\omega_p - Z\Omega]l_\theta - \frac{d\phi}{dr}G_\theta \quad (22)$$

$$\frac{dG_\theta}{dr} = -\gamma\Sigma r^3\Omega l_\theta + \frac{d\phi}{dr}G_\phi \quad (23)$$

$$l_\theta\frac{d\phi}{dr} = \frac{4}{\Sigma c_s^2 r^3\Omega}\left([\alpha\Omega-\gamma]G_\phi + [\omega_p - K\Omega]G_\theta\right) \quad (24)$$

$$\frac{dl_\theta}{dr} = \frac{4}{\Sigma c_s^2 r^3\Omega}\left([K\Omega-\omega_p]G_\phi + [\alpha\Omega-\gamma]G_\theta\right) \quad (25)$$

To the lowest order in the perturbation from the flat disc solution ($G_\theta = G_\phi = \phi = \gamma = 0$, and l_θ =constant, which we set to unity without loss of generality as the equations are homogeneous), we have

$$\frac{dG_\phi}{dr} = \Sigma r^3\Omega[\omega_p - Z\Omega] \quad (26)$$

$$\frac{d\phi}{dr} = \frac{4\alpha}{\Sigma c_s^2 r^3}G_\phi \quad (27)$$

$$\frac{dl_\theta}{dr} = \frac{4}{\Sigma c_s^2 r^3\Omega}[K\Omega-\omega_p]G_\phi \quad (28)$$

$$\frac{dG_\theta}{dr} = \frac{4\alpha G_\phi^2}{\Sigma c_s^2 r^3} - \gamma\Sigma r^3\Omega. \quad (29)$$

This solution is valid as long as $|l_\theta(r)-1| \ll 1$ for all r, $d\phi/dr$ is small enough that the small warp condition $|d\hat{\boldsymbol{l}}/d\ln r| \ll 1$ is satisfied, and the damping rate satisfies $\gamma \ll \alpha\Omega$.

Integrating Eq. (26) [or Eq. (11)] over the entire disc, and taking into account the zero-torque boundary condition, we obtain the global precession frequency of the disc:

$$\omega_p = \frac{\int_{r_{\rm in}}^{r_{\rm out}} d\tilde{r}\Sigma\tilde{r}^3\Omega^2 Z}{\int_{r_{\rm in}}^{r_{\rm out}} d\tilde{r}\Sigma\tilde{r}^3\Omega}. \quad (30)$$

To the lowest order, the disc precesses as a rigid-body at the frequency ω_p, and there is no damping of the warp. For $Z > 0$, the precession will be prograde, while for $Z < 0$ the precession is retrograde (for circumbinary and circumstellar discs, we have $Z < 0$).

The first-order correction to the internal stress $\tilde{\boldsymbol{G}}$ is obtained by integrating Eq. (26), giving

$$G_\phi(r) = \int_{r_{\rm in}}^{r} d\tilde{r}\Sigma\tilde{r}^3\Omega(\omega_p - Z\Omega). \quad (31)$$

The stress is 90^0 out of phase with the warp, linear in the external torque [i.e. in $Z(r)$] and, by construction, vanishes on both boundaries.

We are now free to choose boundary conditions for (l_θ, ϕ), as long as the resulting disc profile is consistent with our perturbative analysis. A good choice is to fix the orientation of the disc at the outer boundary, $l_\theta(r_{\rm out}) = 1, \phi(r_{\rm out}) = 0$. We then integrate Eqs. (27)-(28) to find

$$\phi(r) = \int_{r_{\rm out}}^{r} d\tilde{r}\frac{4\alpha}{\Sigma c_s^2\tilde{r}^3}G_\phi, \quad (32)$$

$$l_\theta(r) = 1 + \int_{r_{\rm out}}^{r} d\tilde{r}\frac{4}{\Sigma c_s^2\tilde{r}^3\Omega}\left(\Omega K - \omega_p\right)G_\phi. \quad (33)$$

We thus have a twist of the disc proportional to the viscosity α, and a small warp due to the external torque. The dimensionless warp $\psi = |\partial\hat{\boldsymbol{l}}/\partial(\ln r)|$ is then easily obtained (reintroducing the scaling of the warp with the misalignment angle of the outer edge of the disc $\beta_{\rm out}$, neglected when we set $l_\theta = 1$):

$$|\psi| = |G_\phi|\frac{4}{\Sigma c_s^2 r^2\Omega}\sqrt{\alpha^2\Omega^2 + (K\Omega-\omega_p)^2}\sin\beta_{\rm out}. \quad (34)$$

This expression will make it easy to check whether the small warp condition $\psi \ll 1$ is satisfied so that the linear theory is valid.

Up to this point, our solution for ω_p and l_θ is formally equivalent to the results derived by Papaloizou & Terquem (1995) in the context of circumstellar discs. By including the effect of finite viscosity α, however, we have also derived the twist of the disc $\phi(r)$ and can now compute the damping rate of the mode γ. Integrating Eq. (29), we find

$$\gamma = \frac{\int_{r_{\rm in}}^{r_{\rm out}} d\tilde{r}\frac{4\alpha G_\phi^2}{\Sigma c_s^2\tilde{r}^3}}{\int_{r_{\rm in}}^{r_{\rm out}} d\tilde{r}\Sigma\tilde{r}^3\Omega}, \quad (35)$$

which is effectively equivalent to what is found at first order when using the expansion of the solution in powers of the tidal potential proposed by Lubow & Ogilvie (2000).

We see that $\gamma \geqslant 0$ for all values of G_ϕ, i.e., the lowest-order warp mode is always damped when considering time-averaged axisymmetric perturbing potentials. A simple physical interpretation of γ can be obtained by integrating the numerator of Eq. (35) by parts and using Eqs. (31)-(32). We find

$$\gamma = \frac{\int_{r_{\rm in}}^{r_{\rm out}} d\tilde{r}\Sigma\tilde{r}^3\Omega(Z\Omega - \omega_p)\phi}{\int_{r_{\rm in}}^{r_{\rm out}} d\tilde{r}\Sigma\tilde{r}^3\Omega}. \quad (36)$$

Here the denominator is the total angular momentum of the disc $L_{\rm disc}$ (up to a factor of 2π). The numerator is the difference between the total torque applied on the disc, and the torque required to maintain the global precession of the disc (up to the same factor of 2π). The existence of this difference is due to the fact that the finite viscosity α twists the disc by an angle ϕ, thus creating a non-zero torque on the disc in the plane defined by the orbital angular momentum of the binary $\mathbf{L}_b$ and that of the disc.

We can similarly infer the back-reaction torque applied by the warped disc onto the binary,

$$\mathbf{T}_{\rm br} = -2\pi\int_{r_{\rm in}}^{r_{\rm out}} d\tilde{r}\Sigma\tilde{r}^3 Z\Omega^2(\hat{\mathbf{e}}_z\times\hat{\boldsymbol{l}}). \quad (37)$$

Recall that $\mathbf{L}_b$ is along $\hat{\mathbf{e}}_z$, while $\hat{\boldsymbol{l}}$ generally deviates from $\mathbf{L}_{\rm disc}$ (the total angular momentum vector of the disc). The term in $\mathbf{T}_{\rm br}$ along the direction $\mathbf{L}_{\rm disc}\times\mathbf{L}_b$ causes $\mathbf{L}_b$ to precess around $\mathbf{L}_{\rm disc}$, while the term in the plane defined by $\mathbf{L}_{\rm disc}$ and $\mathbf{L}_b$ can either cause the binary to align with the disc (for prograde discs) or drive an increase in the misalignment between the disc and the binary (for retrograde discs). The relative importance of the back-reaction torque compared to the "direct" damping effect of the disc inclination depends on the ratio of the angular momenta of the disc and the binary ($L_{\rm disc}$ and L_b). If $L_b \gg L_{\rm disc}$ the disc will align with the binary on a timescale $\sim\gamma^{-1}$. For arbitrary ratio $L_{\rm disc}/L_b$, we must take into account changes to the angular momenta of both the disc and the binary, and alignment occurs on the timescale

$$t_{\rm damp} \simeq \gamma^{-1}(1 + L_{\rm disc}/L_b)^{-1}. \quad (38)$$

We could, in theory, iterate further and compute the

second-order corrections to the warp, stress, and eigenfrequency. However, if the first-order corrections are large enough that this appears warranted, there is no guarantee that this procedure will eventually converge. Solving the eigenvalue problem numerically is then probably a safer option. When the first-order corrections are small, however, we will see that the approximate formulae derived above are accurate enough to give good estimates of the warp and twist of the disc and of the damping timescale of its lowest-order eigenmode.

2.3 Analytical Results for Specific disc Models

The analytical expressions given in Sec. 2.2 are significantly easier to compute than the full numerical solutions to the eigenvalue problem. However, they still require recursive computations of integrals over the whole disc. Here we consider discs with the following power-law profiles:

$$\Sigma(r) = \Sigma_{\rm in}\left(\frac{r}{r_{\rm in}}\right)^{-p}, \quad c_s(r) = c_{\rm in}\left(\frac{r}{r_{\rm in}}\right)^{-c}, \tag{39}$$

$$Z(r) = Z_{\rm in}\left(\frac{r}{r_{\rm in}}\right)^{-z}, \quad K(r) = K_{\rm in}\left(\frac{r}{r_{\rm in}}\right)^{-k}, \tag{40}$$

$$\Omega(r) = \Omega_{\rm in}\left(\frac{r}{r_{\rm in}}\right)^{-3/2}. \tag{41}$$

Substituting these profiles into the relevant expressions of Sec. 2.2, we obtain (where $x = r/r_{\rm in}$)

$$\omega_p = Z_{\rm in}\Omega_{\rm in}\Gamma_p, \tag{42}$$

$$G_\phi(x) = -\Sigma_{\rm in} r_{\rm in}^4 \Omega_{\rm in}^2 Z_{\rm in}\Gamma_G(x), \tag{43}$$

$$l_\theta(x) = 1 - \frac{4Z_{\rm in}}{\delta_{\rm in}^2}(Z_{\rm in}\Gamma_1(x) - K_{\rm in}\Gamma_2(x)), \tag{44}$$

$$\phi(x) = \frac{4\alpha Z_{\rm in}}{\delta_{\rm in}^2}\Gamma_3(x), \tag{45}$$

$$\frac{|\psi|}{\sin\beta_{\rm out}} = \frac{4|Z_{\rm in}|}{\delta_{\rm in}^2} x^{p+2c-2}\Gamma_G(x)\sqrt{\alpha^2 + (K - \frac{\omega_p}{\Omega})^2}, \tag{46}$$

$$\gamma = \frac{4\alpha\Omega_{\rm in}Z_{\rm in}^2}{\delta_{\rm in}^2}\Gamma_I \tag{47}$$

for the precession frequency, internal stress, warp, twist and damping frequency of the eigenmode. In the above, $\delta_{\rm in} = c_{\rm in}/(r_{\rm in}\Omega_{\rm in})$ is the thickness of the disc at its inner edge. The shape functions $\Gamma_{1,2,3,p,G,I}$, which depend only on the shape of the background profiles and on the relative size of the disc $x_{\rm out} = r_{\rm out}/r_{\rm in}$, are given in Appendix A. [1] Their signs are chosen so that $\Gamma > 0$ for circumbinary discs. For convenience, we also plot their value for a few disc profiles important to the study of circumbinary discs ($z = k = 2$, $Z = -K$, $p = 0.5$ or $p = 1$, and $c = 0, 0.2, 0.5$, see discussion below), in Figs. 1-4.

An approximate expression for the mode damping rate γ, based on estimating the energy loss rate due to viscous dissipation in the disc, has previously been proposed in the context of circumstellar discs (using arguments generally applicable to both circumstellar and circumbinary discs) by Bate et al. (2000) for discs of constant thickness ($\delta = H/r$ =constant):

$$\gamma_{\rm Bate} = \frac{\alpha}{\delta^2}\frac{\omega_p^2}{\Omega(r_{\rm out})} = \frac{\alpha Z_{\rm in}^2\Omega_{\rm in}}{\delta^2}\Gamma_p^2 x_{\rm out}^{3/2}. \tag{48}$$

Not surprisingly, our results agree with this expression as far as the general scaling of γ with α, $\delta_{\rm in}$ and $Z_{\rm in}$ is concerned. The actual value of γ can however vary by a factor of a few for moderate-sized discs ($x_{\rm out} \sim 10$), and by more than an order of magnitude for $x_{\rm out} \sim 100-1000$. The approximation used in Bate et al. (2000) only recovers the correct scaling of γ with the size of the disc in the special case $p = 1, c < 0.5$, and does not find the asymptotic behavior $\gamma \to 0$ for an infinitely narrow disc $x_{\rm out} \to 1$ (when $\Gamma_p \to 1$, but $\Gamma_I \to 0$). We will show that our formula agrees much better with the numerical simulations of warped discs, and with the exact solution to the eigenvalue problem.

Our results are also in agreement with the simpler

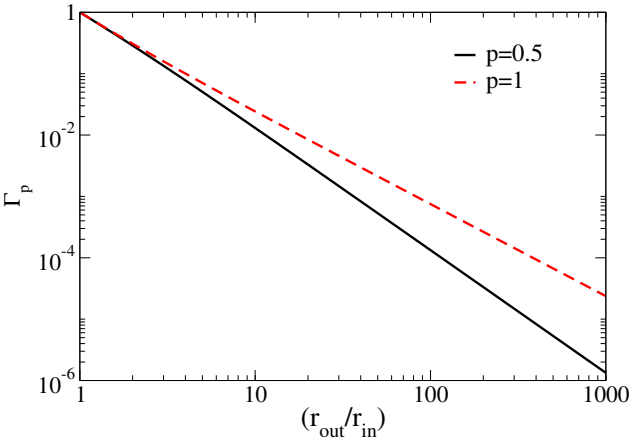

Figure 1. Shape function Γ_p determining the global precession rate of the disc [see eq. (42)] for circumbinary discs with $p = 0.5$ and $p = 1$ (Γ_p is independent of the sound speed profile).

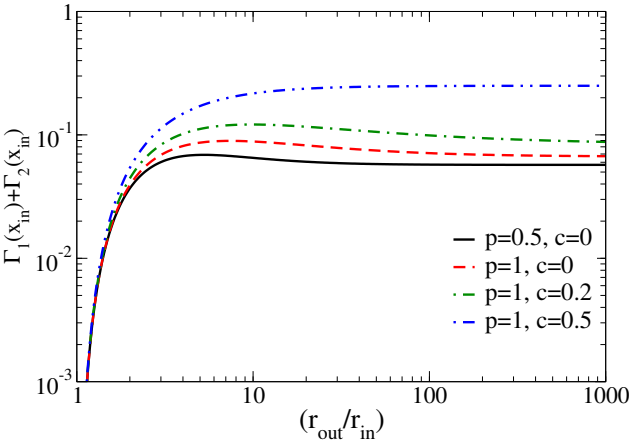

Figure 2. Shape function $\Gamma_1 + \Gamma_2$ determining the warp of the disc [see eq. (44)] for circumbinary discs with $p = 0.5$, $p = 1$ and a constant sound speed, as well as for discs with $p = 1$ and different sound speed profiles $c = 0.2, 0.5$ (a flaring disc and a disc of constant thickness $\delta = H/r$). The functions are evaluated at the inner edge of the disc, in order to provide the total warp of the disc.

[1] We here choose a notation in which the dependency of the shape functions Γ in $x_{\rm out}$ and in the disc profile is implicit, to simplify the equations.

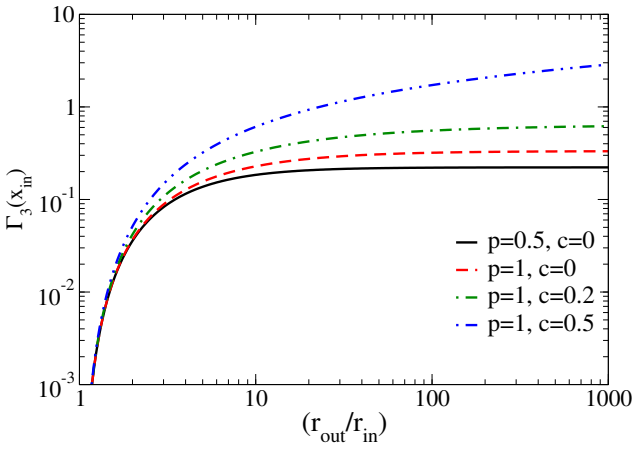

Figure 3. Shape function Γ_3 determining the twist of the disc [see eq. (45)] for the same discs as in Fig. 2. The functions are evaluated at the inner edge of the disc, in order to provide the total twist of the disc

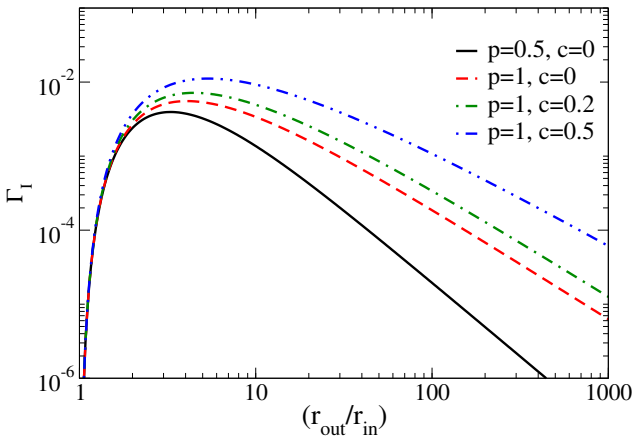

Figure 4. Shape function Γ_I determining the alignment timescale of the disc [see eq. (47)] for the same discs as in Fig. 2.

model that we derived in a previous paper in the limit of $x_{\rm out} \to \infty$ and $\omega_p = 0$ (Foucart & Lai 2013).

2.4 Numerical solutions: disc eigenmodes

Before applying our analytical results to real astrophysical systems, we would like to get an estimate of their accuracy when compared to the numerical solution of the eigenvalue problem given by Eqs. (11)-(14). We use the shooting method to solve the set of 4 complex ODEs, combined with a Newton-Raphson root-solver to find the value of the warp at the disc boundaries and the complex eigenvalue ω. In more details, we assume the boundary conditions $\tilde{l}_x(r_{\rm out}) = 1$, $\tilde{G}_{x,y}(r_{\rm in}) = 0$ and $\tilde{G}_{x,y}(r_{\rm out}) = 0$, and we solve for $\tilde{l}_y(r_{\rm out})$, $\tilde{l}_{x,y}(r_{\rm in})$ and ω using the initial guess $\tilde{l}_y(r_{\rm out}) = i$, $\tilde{l}_{x,y}(r_{\rm in}) = \tilde{l}_{x,y}(r_{\rm out})$, $\omega = 10^{-7}\Omega_{\rm in}$. At each Newton-Raphson iteration, we integrate the 4 complex ODEs from both boundaries, and measure the mismatch between the solutions at the midpoint of the disc. The problem is then reduced to solving for the value of the 4 complex unknowns, $\tilde{l}_y(r_{\rm out})$, $\tilde{l}_{x,y}(r_{\rm in})$ and ω, which satisfy the 4 complex matching conditions at the midpoint of the disc [2]. In general, there is an infinite number of eigenmodes which are solutions of this problem; which one the Newton-Raphson solver converges to depends on the chosen initial guess for the warp on the boundaries and the eigenfrequency. The initial choice made here is convenient for finding the solution closest to the flat disc profile, which has the smallest warp, internal stresses, and damping timescale rate and should thus dominate the long term evolution of the warp. Higher-order modes can be found using the same method if the initial guess is modified appropriately.

We test our analytical results on a sequence of circumbinary disc models with power-law profiles. For a circumbinary disc, we have

$$Z(x) \approx -\frac{3\eta}{4}\left(\frac{a}{r_{\rm in}}\right)^2 x^{-2}, \quad (49)$$

$$K(x) \approx -Z(x), \quad (50)$$

where $\eta = M_1 M_2/(M_1+M_2)^2$ is the symmetric mass ratio of the binary, and a its semi-major axis. The other parameters are set to $p = 1, c = 1/2, \alpha = 0.01, \delta_{\rm in} = 0.1, r_{\rm in} = 2a$. For this choice of c, the condition for the propagation of bending waves $\alpha < H/r$ is satisfied at all radii ($H/r = \delta_{\rm in}$ everywhere). For an equal mass binary ($\eta = 1/4$), we then have $K_{\rm in} = -Z_{\rm in} = 0.047$. The disc precession frequency can, for $x_{\rm out} \gg 1$, be approximated as $\omega_p = 0.035 x_{\rm out}^{-3/2}\Omega_{\rm in}$. By comparison, the timescale for the wave to propagate across the disc is $t_{\rm wave} \sim (0.075\Omega_{\rm in} x_{\rm out}^{-3/2})^{-1} < \omega_p^{-1}$. The disc should thus be able to precess coherently regardless of its size.

According to Eq. (46), the dimensionless warp parameter ψ is maximum for $x \approx 0.6 x_{\rm out}$, where $\psi \approx 0.1 \sin\beta_{\rm out}$. The small warp approximation is thus valid regardless of the value of $\beta_{\rm out}$.

To compare the analytical and numerical solutions, we extract from the numerical results the shape functions $\Gamma_p, \Gamma_I, \Gamma_3(1)$, and $[\Gamma_1(1) + \Gamma_2(1)]$ (we cannot extract separately Γ_1 and Γ_2, as they both contribute to the warp of the disc), and divide them by the analytical values obtained in Appendix A, and plotted in Figs. 1-4. The results are shown in Fig. 5. The first-order analytical approximation recovers the disc profile and the precession timescale to $\sim 10\% - 20\%$ accuracy over a wide range of disc sizes ($x_{\rm out} \sim 5 - 1000$). The damping timescale is recovered to a similar accuracy for small discs ($x_{\rm out} \lesssim 10$), and within $\sim 40\%$ for larger discs.

The warp and twist profiles of the disc as a function of radius are shown in Fig. 6 for a disc with $x_{\rm out} = 100$. We see that the general shape of the profile is also recovered with good accuracy. The disc is warped in two distinct regions, due to the different dependence of the shape functions Γ_1 and Γ_2 on the radius of the disc: at small radii, where the non-Keplerian contributions to the warp ($\propto \Gamma_2$) are maximum, and at larger radii, where the contributions to the warp due to the external torque ($\propto \Gamma_1$) dominate.

[2] Note however that we can always make use of the fact that $\tilde{l}_y = i\tilde{l}_x$ for the modes that we are interested in - so that in practice the number of independent variables and equations could be reduced by a factor of 2. Our code solves the full system of equations because it was developed in a more general framework in which the two families of modes $W_\pm$ might be distinct (see e.g. Lubow & Ogilvie 2000).

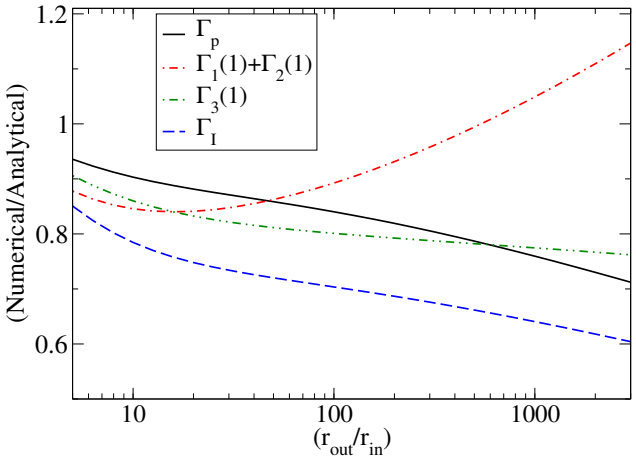

Figure 5. The ratio of the numerical and analytical values of the shape functions Γ_p, $[\Gamma_1(1)+\Gamma_2(1)]$, $\Gamma_3(1)$ and Γ_I for a misaligned circumbinary disc. The disc is assumed to follow a power-law density profile with $p = 1$, is of constant dimensionless thickness $\delta = H/r = 0.1$, and has a viscosity parameter of $\alpha = 0.01$. The outer edge of the disc is varied between $r_{\rm out} = 5r_{\rm in}$ and $r_{\rm out} = 3000r_{\rm in}$. The central binary has equal mass components, and a semi-major axis $a = 0.5r_{\rm in}$.

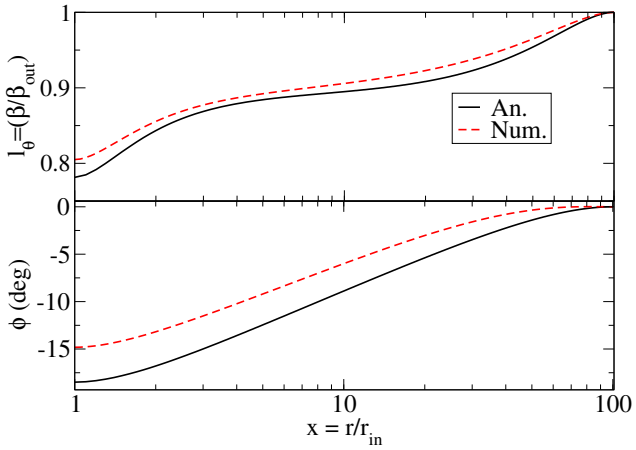

Figure 6. Inclination (top) and twist (bottom) profiles for a circumbinary disc with $\alpha = 0.01$, $\delta = 0.1$, $p = 1$, $c = 0.5$, $r_{\rm out} = 100r_{\rm in}$, $\eta = 0.25$ and $r_{\rm in} = 2a$. The solid black lines show our approximate analytical solution, and the dashed red lines the exact numerical solution.

The twist, on the other hand, has a single component due to the finite viscosity of the disc ($\propto \Gamma_3$).

Finally, the values of the shape functions are plotted on Fig. 7 (see also Sec. 3.1 for more discussion). Figure 7 also shows the damping rate that would be expected from the approximate formula derived in Bate et al. (2000). While the approximate formula performs relatively well for $x_{\rm out} \sim 5-10$, it becomes increasingly unreliable for larger discs (and for different choices of the parameters p and c, the error in the approximate formula of Bate et al. can be even larger).

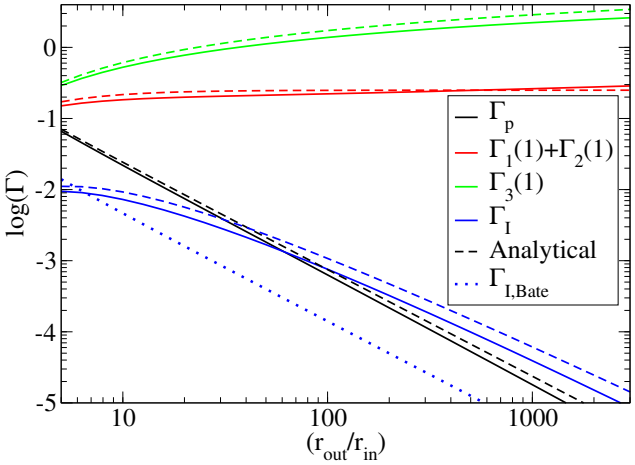

Figure 7. Numerical (solid lines) and analytical (dashed lines) values of the logarithm of the shape functions Γ_p, $[\Gamma_1(1)+\Gamma_2(1)]$, $\Gamma_3(1)$ and Γ_I for the same configuration as in Fig. 5. The dotted line shows the damping coefficient Γ_I corresponding to the approximate formula derived in Bate et al. (2000).

3 APPLICATION TO CIRCUMBINARY DISCS

3.1 Fiducial disc Model

We can now use the results of the previous section to study the properties of misaligned circumbinary discs. For concreteness, we first consider discs with a constant thickness H/r and a density profile which approximately follows a power-law with $p = 1$. Because the shape functions [Γ's in Eqs. (42)-(47)] depend only on $r_{\rm out}/r_{\rm in}$ and on the assumed disc profile, the other parameters can be varied at will without changing the value of the Γ functions — as long as the small warp approximation remains valid. Here we consider prograde discs with $r_{\rm out} \gg r_{\rm in}$, and will discuss modifications for retrograde discs in Sec. 3.3.

The global precession period of the disc is

$$P_p = 20200 \left(\frac{r_{\rm out}}{100{\rm AU}}\right)^{3/2} \frac{1}{4\eta} \left(\frac{r_{\rm in}}{2a}\right)^2 \left(\frac{2M_\odot}{M}\right)^{1/2} {\rm yrs} \quad (51)$$

where $M = M_1 + M_2$ is the mass of the binary. The travel time of bending waves across the disc is

$$t_{\rm wave} = 1500 \left(\frac{r_{\rm out}}{100{\rm AU}}\right)^{3/2} \frac{0.1}{\delta_{\rm in}} \left(\frac{2M_\odot}{M}\right)^{1/2} {\rm yrs}, \quad (52)$$

which is shorter than P_p for a reasonable disc thickness, justifying global disc precession. For comparison, the viscous timescale in the disc $t_\nu = r^2/(\alpha_0 H^2 \Omega)$ is

$$t_\nu = 1.1 \times 10^6 \left(\frac{r}{100{\rm AU}}\right)^{3/2} \left(\frac{2M_\odot}{M}\right)^{1/2} \frac{0.01}{\alpha_0} \left(\frac{0.1}{\delta_{\rm in}}\right)^2 {\rm yrs}, \quad (53)$$

which is significantly longer for our standard disc parameters. Note that we explicitly differentiate between the viscosity parameter α_0 responsible for the viscous evolution of the disc density profile and the viscosity parameter α responsible for the damping of disc warp.

The relative change in the warp across the whole disc,

$\delta l_\theta = |1 - l_\theta(1)|$, is

$$\begin{aligned}\delta l_\theta &= 0.88\left[\Gamma_1(1)+\Gamma_2(1)\right](4\eta)^2\left(\frac{2a}{r_{\rm in}}\right)^4\left(\frac{0.1}{\delta_{\rm in}}\right)^2 \\ &\approx 0.2(4\eta)^2\left(\frac{2a}{r_{\rm in}}\right)^4\left(\frac{0.1}{\delta_{\rm in}}\right)^2, \end{aligned} \quad (54)$$

where in the second line we have used the fact that $\Gamma_1(1)+\Gamma_2(1)$ is nearly independent of $x_{\rm out}$ (see Fig. 7). The strong dependence of the warp on the location of the inner radius of the disc is noteworthy. If the inner edge of the disc was closer to the binary, the small warp approximation would break down.

The twist across the disc is given by

$$\phi(1) = -24^\circ\frac{\alpha}{0.01}(4\eta)\left(\frac{2a}{r_{\rm in}}\right)^2\left(\frac{0.1}{\delta_{\rm in}}\right)^2\frac{\Gamma_3(1)}{2}. \quad (55)$$

In contrast with the disc warp, the twist has a non-negligible dependence on the size of the disc, since $\Gamma_3(1)$ varies by about an order of magnitude between $x_{\rm out}=5$ and $x_{\rm out}=3000$ (see Fig. 7). For large discs ($x_{\rm out}\sim 100-3000$), we have $\Gamma_3(1)\sim 2$, hence the scaling chosen in our twist expression given above. However, narrower discs can have much smaller twists, of order of a few degrees.

For the disc profile considered in this section, Eq. (46) shows that the maximum of the dimensionless warp $\psi_{\rm max}$ is largely independent of the location of the outer edge of the disc, and is given by

$$\psi_{\rm max} = 0.1(4\eta)^2\left(\frac{2a}{r_{\rm in}}\right)^4\left(\frac{0.1}{\delta_{\rm in}}\right)^2\sin\beta_{\rm out} \quad (56)$$

if $\alpha \lesssim Z(1.4)$ (i.e. if we can neglect α in Eq. [46]). The condition $|d\ln\hat{\boldsymbol{l}}/dr|<1$ is thus easily satisfied. The stronger constraint $|d\ln\hat{\boldsymbol{l}}/dr|<H/r$ suggested by the numerical work of Sorathia et al. 2013a is marginally satisfied for our fiducial disc parameters. For thinner discs, nonlinear effects might thus cause the damping of the inclination to be faster than what the linear theory predicts.

Finally, we can compute the alignment timescale of the disc and the binary:

$$t_{\rm damp} = \gamma^{-1}\left[1+\frac{2M_{\rm disc}}{3M}\left(\frac{a}{r_{\rm out}}\right)^{1/2}\right]^{-1}, \quad (57)$$

$$\begin{aligned}\gamma^{-1} &= 13000\frac{1}{x_{\rm out}^{3/2}\Gamma_I}\left(\frac{\delta_{\rm in}}{0.1}\right)^2\left(\frac{0.01}{\alpha}\right)\left(\frac{2M_\odot}{M_b}\right)^{1/2} \\ &\quad\times\left(\frac{r_{\rm out}}{100{\rm AU}}\right)^{3/2}(4\eta)^{-2}\left(\frac{r_{\rm in}}{2a}\right)^4{\rm yrs}. \end{aligned} \quad (58)$$

This means that, for $r_{\rm out}\gtrsim 100$AU, a circumbinary disc of constant thickness $\delta=0.1$ and viscosity $\alpha=0.01$ will align on a timescale comparable to its global precession timescale, and much shorter than its expected lifetime. This can easily be understood from the fact that most of the disc angular momentum is at large radii, while most of the torque exerted by the binary on the disc is applied at small radii. The torque is perpendicular to the local direction of the disc angular momentum, which is rotated by an angle $\sim\phi(1)$ with respect to the total angular momentum of the disc. A component of order $(\sin\phi)T$ of the total torque T will thus attempt to align the angular momentum of the disc, while the precession is due to a torque of order $(\cos\phi)T$. For our nominal value of $\phi(1)=24^\circ$ at the inner edge of the disc, about $0.4T$ goes towards aligning the disc instead of driving precession.

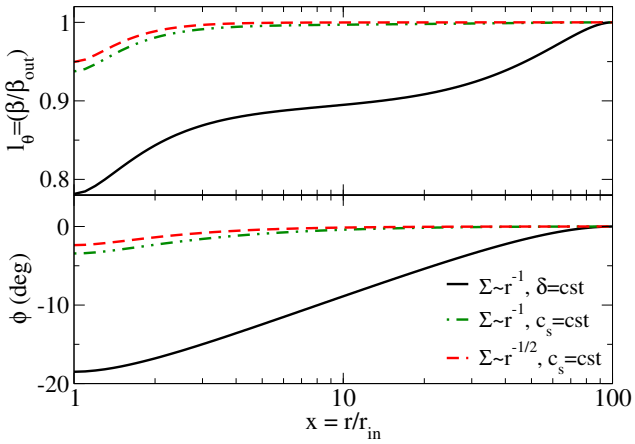

Figure 8. Warp (top) and twist (bottom) profiles for 3 different choices of power-law profiles for discs which otherwise have the same parameters as in Fig. 6. Two of the profiles have $p=1$ and either a constant sound speed ($c=0$) or a constant H/r ($c=0.5$), while the third has $p=0.5$ and a constant sound speed.

From the above results we see that, for the fiducial disc profile considered here, an inclined circumbinary disc can survive for a significant fraction of its viscous evolution timescale only if one of the following conditions is met:

- A low effective viscosity $\alpha \ll \alpha_0$. This appears unlikely; if anything, the growth of parametric instabilities could cause $\alpha \gg \alpha_0$ for misalignments greater than a few degrees (see Sec. 5).
- A thick disc $\delta \gtrsim 0.3$. This is also unlikely for protoplanetary discs.
- A small symmetric mass ratio $\eta \ll 1/4$. This should be rare as η varies slowly with the mass ratio $q=M_2/M_1$ of the binary for $q\sim 1$ (to gain a factor of 3 in η, one needs a binary with a mass ratio of 1:10)
- A large binary eccentricity. This would lead to disc truncation at $r_{\rm in}\gtrsim 4a$ (Artymowicz & Lubow 1994). Given the strong dependance of the damping timescale in the ratio $r_{\rm in}/a$, this would modify the damping timescale by about an order of magnitude.

3.2 Dependence on the disc profile

The power-law surface density profile $\Sigma\propto r^{-p}$ with $p=1$ considered in the previous subsection provides only an approximate description of protoplanetary discs. Other density profiles are possible (e.g., Williams & Cieza 2011). There is also uncertainty on the temperature profile of the discs. Observations suggest that protoplanetary discs have a 'flaring' profile, where H/r grows with radius. This corresponds to a sound speed profile $c_s(r)\propto r^{-c}$, with $0\leqslant c\leqslant 0.5$ (with preferred value $c\sim 0.2$, or $H\propto r^{1.3}$). Here we examine how different disc profile parameters (p,c) affect the evoluton of disc warp and misalignment.

Qualitatively, a flaring disc has large $\delta=H/r$ for $r\gg r_{\rm in}$, thus decreasing the warp and twist of the disc at large radii. A flaring disc is thus nearly flat at large radii, while its behavior is mostly unmodified for $r\sim r_{\rm in}$. Figure 8 shows

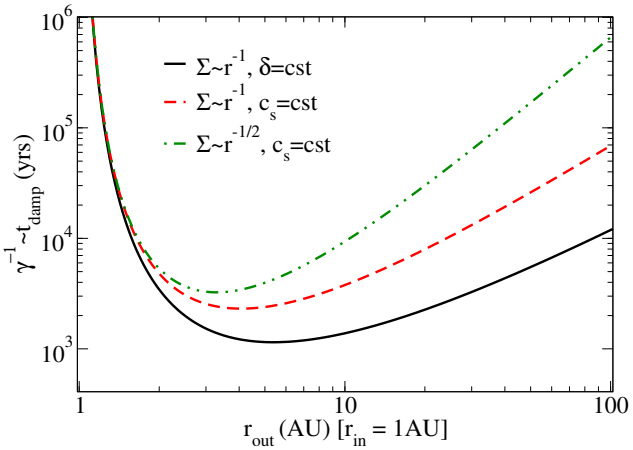

Figure 9. disc inclination damping timescale as a function of the radial aspect ratio of the disc $x_{\rm out} = r_{\rm out}/r_{\rm in}$ for the three choices of power-law profiles considered in Fig. 8. The other parameters are $\alpha = 0.01$, $\delta_{\rm in} = 0.1$, $\eta = 0.25$, $M = 2M_\odot$ and $r_{\rm in} = 2a = 1$AU.

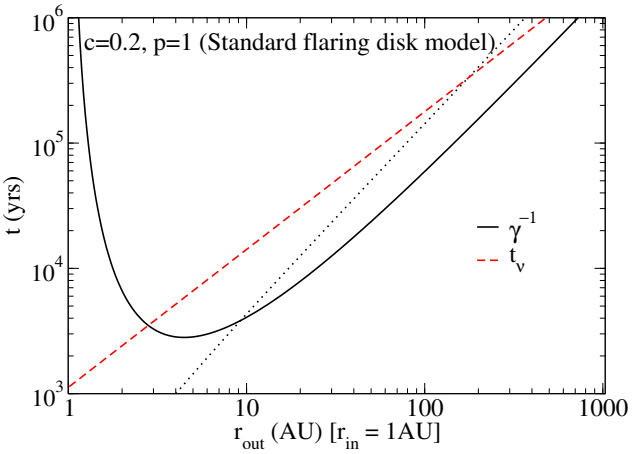

Figure 10. Timescales for the damping of the inclination (solid black line) and the viscous evolution (dashed red line) of a typical flaring disc profile ($c = 0.2$, $p = 1$). The other parameters of the system are $\alpha = \alpha_0 = 0.01$, $\delta_{\rm in} = 0.1$, $\eta = 0.25$, $M = 2M_\odot$ and $r_{\rm in} = 2a = 1$AU. The dotted black line show the result based on the approximate formula of Bate et al. (2000).

an example of this behavior for the relatively extreme case $c = 0$ (constant sound speed, or $H \propto r^{3/2}$). Because the disc is nearly flat for $r \gtrsim 5r_{\rm in}$, the total twist and warp are about a factor of 4 smaller than in the $c = 0.5$ case (constant δ). This is reflected in the inclination damping timescale, shown in Fig. 9: as the damping is due to the misalignment between the outer and inner edges of the disc, a flaring disc can remain inclined for a significantly longer time than a disc of constant δ. For $x_{\rm out} \sim 100$, going from $c = 0.5$ to $c = 0$ increases the damping timescale by a factor of ~ 6. We expect most protoplanetary discs to lie in between these two limits.

The disc flaring effect is illustrated in Fig. 10 for a disc model with $c = 0.2$. We see that for our standard choice of parameters, the damping timescale for the inclination is $\sim 20\% - 30\%$ of the viscous evolution timescale t_ν for $x_{\rm out} \sim 10 - 100$. There is thus a class of acceptable disc parameters for which $t_{\rm damp} \sim t_\nu$. Rapid damping of the inclination does however remain the most likely outcome. Indeed, $\delta_{\rm in} \sim 0.1$ is probably optimistic for such a flaring disc, and $t_{\rm damp}/t_\nu \propto \delta_{\rm in}^4$. Additionally, $\alpha_0 \ll 0.01$ is quite likely in the dead zones, but the same is probably not true for α (see Sec. 5). A combination of these effects is likely to lead to the observed $t_\nu \sim 10^{6-7}$yrs for $r_{\rm out} \sim 100$AU without causing as much of a modification in $t_{\rm damp}$ – thus leading to $t_{\rm damp} \sim (0.005 - 0.05)t_\nu$ for our standard parameters. Conversely, this means that the observation of a significant inclination in a circumbinary disc can provide significant constraints on the age and parameters of the system.

The density profile of the disc has a smaller effect on its warp and twist profiles, as both the torque applied on an annulus of the disc and the angular momentum of that annulus are proportional to its surface density. This is shown in Fig. 8 for a disc with $p = 0.5$, $c = 0$. The effect on the inclination damping timescale is much more significant. Indeed, a shallower disc profile ($p < 1$) has a larger fraction of its angular momentum in the outer region of the disc. Thus, it is harder for the torques applied on the smaller amount of material available at small radii to affect the global evolution of the disc. Accordingly, both the precession timescale and the damping timescale are larger (see Fig. 9). For $x_{\rm out} \gg 1$ and $p + c < 1.5$, these scale as $\omega_p \propto \gamma \propto x_{\rm out}^{p-5/2}$. A shallow disc profile, although less likely than a flaring disc, thus provides another pathway to increase the timescale over which the disc's inclination is damped.

3.3 Retrograde circumbinary discs

Most of the results discussed in the previous sections can be directly applied to retrograde circumbinary discs, as long as the misalignment between the orbital angular momenta of the disc and the binary remains small. There are however a few important distinctions when attempting to determine the long term evolution of retrograde discs. The first is that, because there are no Lindblad resonances in these discs, we expect the inner edge of the disc to be closer to the binary. This will result in shorter precession ($\propto r_{\rm in}^2$) and damping ($\propto r_{\rm in}^4$) timescales, larger twists ($\propto r_{\rm in}^{-2}$) and warps ($\propto r_{\rm in}^{-4}$), and faster growth of parametric instabilities. A low mass retrograde disc will thus rapidly reach a nearly counter-aligned configuration.

The second difference is that the back-reaction torque on the binary has the effect of increasing the misalignment of the disc with respect to the counter-aligned equilibrium configuration. This means that if the angular momentum of the disc is larger than the angular momentum of the binary, the misalignment angle is driven towards 90° and might eventually switch to a prograde configuration. The details of this process have been studied under fairly general assumptions by King et al. (2005). They find that the disc will eventually become prograde if $\cos\theta > -L_{\rm disc}/(2L_b)$.

4 MISALIGNED CIRCUMSTELLAR DISCS

The properties of misaligned circumbinary discs can, in the framework presented here, easily be contrasted with those of circumstellar discs in binary systems, as long as we neglect potential resonances between eigenmodes of the disc

and the time-dependent, $m = 2$ component of the perturbing potential (see the numerical results of Lubow & Ogilvie 2000).

The time-averaged potential produced by an external binary companion on a misaligned circumstellar disc tends to make the disc precess, with the corresponding functions $Z(r)$ and $K(r)$ [see Eqs. (15)-(16)] given by

$$Z(r) = -K(r) \approx -\frac{3q}{4}\left(\frac{r}{a}\right)^3, \tag{59}$$

where $q = M_2/M_1$, $M_1 = M_\star$ is the mass of the central star and M_2 is the companion mass. While the warping of a circumbinary disc is mostly due to torques applied at the inner edge of the disc, the opposite is true for a circumstellar disc. In fact, as soon as the radial aspect ratio of the disc is large enough ($x_{\rm out} \gtrsim 10$), the location of the disc inner edge becomes largely irrelevant. The global precession frequency of the disc is then

$$|\omega_p| = \frac{3}{8}\frac{q}{(1+q)^{1/2}}\left(\frac{5-2p}{4-p}\right)\left(\frac{r_{\rm out}}{a}\right)^{3/2}\Omega_b. \tag{60}$$

For $r_{\rm out} \sim a/3$ (typical of the truncation radius of a circumprimary disc due to the influence of the secondary, see Artymowicz & Lubow 1994) and $q \sim 1$, the disc precesses on a timescale a few times larger than the binary orbital period. The disc warp, twist and damping timescale can be computed using the expressions given in Section 2.2. For $p = 1$ and $c = 0.5$ (constant δ), we find

$$\delta l_\theta \approx -0.01\left(\frac{0.1}{\delta}\right)^2 q^2\left(\frac{3r_{\rm out}}{a}\right)^6, \tag{61}$$

$$\phi(1) \approx 0.01\left(\frac{\alpha}{0.01}\right)\left(\frac{0.1}{\delta}\right)^2 q\left(\frac{3r_{\rm out}}{a}\right)^3, \tag{62}$$

$$\frac{\gamma}{\Omega_b} \approx 1.5\times10^{-4}\left(\frac{\alpha}{0.01}\right)\left(\frac{0.1}{\delta}\right)^2\frac{q^2}{(1+q)^{1/2}}\left(\frac{3r_{\rm out}}{a}\right)^{9/2} \tag{63}$$

We see that circumprimary discs generally have very small warps ($\lesssim 1\%$). Circumsecondary discs have higher mass ratios $q > 1$, but are also truncated at a smaller radius (Artymowicz & Lubow 1994) and will thus avoid significant warping. In contrast to circumbinary discs, the misalignment of a circumstellar disc also damps on a timescale much longer than the precession timescale or even the viscous timescale. It is thus much more natural to expect misaligned circumstellar discs than misaligned circumbinary discs. Furthermore, in circumstellar discs, resonances can drive a growth of the disc inclination for some specific choices of the ratio $r_{\rm out}/a$ (see Lubow & Ogilvie 2000).

Our analytical result for γ matches the numerical solution of Lubow & Ogilvie (2000) to high accuracy (if we adopt the same disc parameters: $p = 0.5$, $c = 0.5$, for which the numerical factor in Eq. (63) is 10^{-4} instead of 1.5×10^{-4}). This is not surprising given that we are starting from the same system of equations and that the assumption of linear warps is more accurate for circumstellar discs than circumbinary discs.[3] Both the results of Lubow & Ogilvie (2000) and those presented here show damping timescales significantly shorter than what would be found using the approximate formula of Bate et al. (2000), by up to an order of magnitude in the range of parameters considered here.

[3] Note, however, that we define the effective scaleheight H through $P = \Sigma\Omega_z^2H^2$, as in Lubow et al. (2002), while it is defined as $P = \Sigma\Omega_z^2H^2/(2n+3)$ in Lubow & Ogilvie (2000), where n is the polytropic index of the fluid. Hence, for the $n = 3/2$ polytrope used in Lubow & Ogilvie (2000), H should be modified by a factor of $\sqrt{6}$ when comparing their results to ours.

5 PARAMETRIC INSTABILITIES

5.1 Conditions for the growth of parametric instabilities

The bending waves by which warps propagate in discs with $H/r \gtrsim \alpha$ are associated with strongly shearing epicyclic motions, whose velocity is proportional to the distance above the mid-plane of the disc (Paploizou & Pringle 1983). When those velocities become close to the sound speed in the disc at some characteristic height $z \sim H$, Gammie et al. (2000) have shown that the internal shearing motions induced by the bending waves are locally unstable to parametric instabilities on a timescale of order the orbital period of the disc. Even when those velocities are subsonic, the instabilities grow on a timescale H/v' (where v' is the velocity of the shearing motions for $z \sim H$) as long as this growth rate is faster than the viscous damping timescale H^2/ν. This translates to the condition

$$|\psi| \geqslant \max\left(A_1\left|q-\frac{3}{2}\right|\alpha, A_2\alpha^2\right), \tag{64}$$

where $q = -d(\ln\Omega)/d\ln r$ and (A_1, A_2) are numerical coefficients expected to be of order unity (Ogilvie & Latter 2013). The conditions under which this occurs in binary systems were first studied by Bate et al. (2000), with the objective of studying circumstellar discs. They estimated v' from the internal stress $\mathbf{G}$ in the disc. More recently, Ogilvie & Latter (2013) have presented the first detailed study of the linear growth of these parametric instabilities, by performing numerical simulations in the warped shearing sheet formalism. For isothermal and quasi-Keplerian discs, they find $A_2 \approx 65$ and $A_1 \approx 45$ (using $q = 1.6$). These results should be taken with some caution, as they are only valid for $\psi \lesssim 0.01$ and likely depend on the vertical profile of the disc. However, they are probably the best estimate currently available when trying to determine whether a given disc profile is susceptible to the growth of parametric instabilities.

From these results, it is clear that in many discs parametric instabilities can grow even when the small warp condition $\psi \ll 1$ is satisfied. They could thus play a significant role in the long term evolution of the disc. However, the consequences of the growth of these instabilities on the behavior of the disc are not known at present. One reasonable assumption is that the warp would then be damped on a timescale comparable to the growth timescale of the instabilities (Gammie et al. 2000, Bate et al. 2000), in which case the parametric instabilities would effectively act as a lower bound on the viscosity parameter α entering the equations for the propagation of bending waves in the disc. That bound would then depend on the maximum value of ψ, and roughly follow Eq. (64). If this is the case, the parametric instabilities could significantly affect the damping timescale of the warp in many relevant astrophysical configurations (Bate et al. 2000; see also the following subsections).

5.2 Effects on Circumbinary discs

By combining the local prescription for the growth of the parametric instability of Ogilvie & Latter (2013) and our calculation for the dimensionless warp ψ in circumbinary discs, we can now obtain an improved estimate of the region of parameter space in which this instability would grow. If we consider the typical 'flaring disc' model used in Sec. 3.2 and Fig. 10 (with $c = 0.2$, $p = 1$), we find the maximum dimensionless warp

$$\psi_{\rm max} \approx 0.09(4\eta)^2 \left(\frac{2a}{r_{\rm in}}\right)^4 \left(\frac{0.1}{\delta_{\rm in}}\right)^2 \sin\beta_{\rm out}. \qquad (65)$$

The condition for the growth of parametric instabilities is thus

$$\sin\beta_{\rm out} \gtrsim 0.07 \left(\frac{\alpha}{0.01}\right)^2 (4\eta)^{-2} \left(\frac{2a}{r_{\rm in}}\right)^{-4} \left(\frac{0.1}{\delta_{\rm in}}\right)^{-2}, \quad (66)$$

or $\beta_{\rm out} \gtrsim 4^\circ$ for our standard disc parameters.

Ogilvie & Latter (2013) find that the growth rate of the parametric instability for ψ only $\sim 20\% - 50\%$ larger than at the onset of instability is already $\gtrsim 0.01\Omega$ (for $\alpha \sim 0.005 - 0.01$). If, as in Bate et al. (2000) we assume that the effect of these instabilities is to damp the inclination of the disc on the growth timescale of the instability, we would expect an effective viscosity of at least $\alpha \sim 0.01$ for any disc inclined by more than a few degrees. For standard circumbinary discs, we would then expect the inclination to decay to $\beta_{\rm out} \ll 1^\circ$ within about 10^5yrs. After that, the inclination would evolve on a longer (viscous) timescale (if the effective viscosity is then $\alpha \ll 0.01$).

We note that the effects of the local parametric instabilities on the global effective viscosity α are still speculative, and that the inclination damping from the growth of the parametric instabilities remains uncertain. However, as shown in previous section, even without taking parametric instabilities into account, we generally get $t_{\rm damp} \ll t_\nu$. Damping of the inclination on a timescale much shorter than the lifetime of the disc is thus expected to be the norm even if the parametric instabilities do not significantly affect the evolution of the inclination.

5.3 Effects on Circumstellar discs

We can now perform an identical calculation for circumstellar discs. Using a constant thickness profile ($p = 1$, $c = 0.5$), we get a maximum dimensionless warp

$$\psi_{\rm max} \approx 0.02q^2 \left(\frac{0.1}{\delta}\right)^2 \left(\frac{3r_{\rm out}}{a}\right)^6 \sin\beta_{\rm out} \qquad (67)$$

for $\alpha \lesssim 0.025q(r_{\rm out}/a)^3$ and would predict the growth of parametric instabilities for

$$\sin\beta_{\rm out} \gtrsim 0.33q^{-2} \left(\frac{\alpha}{0.01}\right)^2 \left(\frac{0.1}{\delta}\right)^{-2} \left(\frac{3r_{\rm out}}{a}\right)^{-6} \qquad (68)$$

or $\beta_{\rm out} \gtrsim 20^\circ$ for our fiducial parameters[4]. The maximum inclination also generally becomes larger for more asymmetric binaries or eccentric systems. We can for example consider a system with $q = 1/2$, and choose the outer radius of the disc to be $r_{\rm out} = 0.4a$ (roughly the expected value for a circular binary, according to Artymowicz & Lubow 1994), and find that parametric instabilities grow for $\beta_{\rm out} \gtrsim 30^\circ$.

In a previous analysis, Bate et al. (2000) suggested that parametric instabilities could damp the inclination of circumstellar discs to within an angle of order H/r with respect to the binary orbital plane (or $\beta_{\rm out} \sim 5^\circ$ for $\delta = 0.1$) on a dynamical time. Their analysis was based on a rough estimate of the total internal stress in the disc. Our calculations based on the local properties of the disc are significantly more favorable for the survival of large inclinations than the result of Bate et al. (2000). Although our understanding of parametric instabilities is insufficient to draw definite conclusions at this point, our results still provide evidence that even if we take into account parametric instabilities, circumstellar discs are likely to be able to maintain large misalignments on timescales comparable to their viscous lifetimes.

6 KH 15D AS A TRUNCATED PRECESSING DISC

In this section, we compare our analytic results to the 1D simulations of Lodato & Facchini (2013) (hereafter LF), who presented numerical models for the KH 15D system. The pre-main sequence binary KH 15D shows an unusual light curve, which has been interpreted as the result of a narrow precessing disc around the binary (Winn et al. 2004, Chiang & Murray-Clay 2004). The system exhibits deep eclipses occurring at a period of 48.35days and lasting $\sim$ 1 day. Radial velocity measurements indicate the binary component masses of $M_1 \sim M_2 \sim 0.5M_\odot$ and orbital eccentricity $0.68 < e < 0.80$ (Johnson et al. 2004). The model of Chiang & Murray-Clay (2004) gives the disc precession period of 2770 yrs (with $M_1 = M_2 = 0.5M_\odot$ and binary separation $a = 0.26$AU).

LF studied two numerical models for the KH 15D disc system. Both have the disc parameters $r_{\rm in} = 4a$ (due to the large eccentricity of the binary), $\delta_{\rm in} = 0.1$, $\alpha = 0.05$, and $c = 3/4$. Their surface density profiles have index $p = 0.5$ and $p = 1$, with the corresponding outer disc radii $x_{\rm out} = 6.71$ and $x_{\rm out} = 9$, respectively. The outer edge of the discs are chosen in order to recover the desired precession period.

We first verify that our model for the profile and evolution of the disc warp agrees with the numerical results obtained by LF. The main results are listed in Table 1, where we give the precession period, total warp, and damping timescale obtained by LF, as well as our results using both the approximate analytical method and the explicit numerical computation of the disc eigenmode. We see that the two numerical methods agree extremely well, with the worst disagreement being on the damping timescale of the $p = 0.5$ model ($\sim 20\%$, while other quantities agree to within a few percents). The approximate analytical model gives equivalently good results for the precession and damping timescales, but perform more poorly for the total disc warp ($\sim 50\%$ error). The reason for this larger error can be easily understood if we also compute the twists, which are 8° and 14° for $p = 0.5$ and $p = 1$ respectively. This means that the twist modifies $\hat{\boldsymbol{l}}$ by $15\% - 25\%$, while the warp is only

[4] For larger viscosities, these scalings are modified. But by that point all inclination angles are stable against the growth of parametric instabilities and inclination damping is dominated by the damping rate given in Eq. (63)

Table 1. disc models for the KH 15D object. For each parameter, we list the values obtained by Lodato & Facchini (2013) using 1D numerical simulations[Num. Sim. (LF)], our numerical results obtained by solving for the lowest order eigenmode of the disc [Num. Eigen.], and the results of the approximate analytical formulae obtained in Appendix A [Analytical]. The warp for the $p = 1/2$ model of LF is taken from Fig.2 of LF, not Table I, as the table lists an incorrect value of the warp (S. Facchini, private communication)

	Num. Sim. (LF)	Num. Eigen.	Analytical
$p = 1/2$ model			
Prec. Period	2670yrs	2800yrs	2764yrs
Warp δl_θ	0.018	0.018	0.013
$t_{\rm damp} = \gamma^{-1}$	4744yrs	5704yrs	5576yrs
$p = 1$ model			
Prec. Period	2680yrs	2861yrs	2769yrs
Warp δl_θ	0.040	0.040	0.024
$t_{\rm damp} = \gamma^{-1}$	3012yrs	3051yrs	2918yrs

a $2\% - 4\%$ effect. Accordingly, the second order terms in the twist, which we have neglected in the computation of the warp, can significantly affect the warp. Note that if we choose $\alpha \lesssim 0.01$, then the approximate analytical method agrees with the eigenmode analysis much better, as shown in Sec. 2.4.

We can now go further and consider the potential influence of parametric instabilities. For the disc to survive multiple precession periods without aligning with the binary, the viscosity needs to be significantly smaller than $\alpha = 0.05$. LF estimate that $\alpha < 0.005$ is required, assuming the expected linear relation $t_{\rm damp} \propto \alpha^{-1}$. Then we have $\psi_{\rm max} \sim 0.009 \sin\beta$ for the $p = 0.5$ model and $\psi_{\rm max} \sim 0.016 \sin\beta$ for the $p = 1$ model. For $\alpha = 0.005$, parametric instabilities will thus develop for $\beta > 10^\circ$ (resp. 5°) for the $p = 0.5$ (resp. $p = 1$) model. In the Chiang & Murray-Clay (2004) models, inclinations of $\sim 10^\circ - 20^\circ$ are required to explain the observation. If the parametric instabilities damp the inclination of the disc, some fine tuning of the disc parameters is needed to (i) maintain solid body precession for multiple precession periods, (ii) avoid fast damping due to parametric instabilities and (iii) maintain a significant disc inclination. For $\alpha \sim 0.005$, these models remain possible, with damping timescales of order of $10 - 20$ precession periods. Considering the uncertainties related to the effects of the parametric instabilities on the long term evolution of the disc, this consideration cannot rule out the precessing disc model for KH 15D. But there are certainly mild tensions between that model and the idea that the warp is damped on the growth timescale of parametric instabilities.

7 DISCUSSION AND CONCLUSION

In this paper, we have presented analytical calculations for the long-term evolution of inclined/warped accretion discs under the influence of an axisymmetric perturbing potential. Such evolution is governed by the combined effects of disc bending waves and viscous dissipation. Our calculations can be applied to misaligned circumbinary and circumstellar discs in protostellar systems, as well as to other astrophysical discs (such as discs formed in neutron star binary mergers and in tidal disruption events). In particular, we have derived approximate expressions for the global precession rate and the disc alignment timescale due to viscous dissipation, as well as expressions for the disc warp and internal stress profiles. Our results build on the analysis performed by Papaloizou & Terquem (1995) for inviscid circumstellar discs, and the formulation of the bending wave equations with finite viscosity as an eigenvalue problem by Lubow & Ogilvie (2000). Our approximate analytic results by-pass the much more time-consuming simulations of the evolution of disc warps, as well as numerical calculations of warp eigenmodes. In essence, our analytic solution corresponds to the lowest-order eigenmode, which dominates the long-term evolution of the disc warp and inclination. We have compared our results to previous numerical calculations (when available) and found good agreement in general. Our analytic results are useful for various applications and also provide insights into the disc warp evolution under various conditions/parameters.

We have applied our results to inclined/warped circumbinary discs. For the viscosity parameter $\alpha \sim 0.01$ (and typical protoplanetary disc parameters), we find that the alignment timescale of the disc is comparable to its global precession timescale, but much shorter than its viscous evolution timescale. For the inclination to survive for a significant fraction of the disc lifetime, we need either a high binary eccentricity or an asymmetric binary, in which case the inner edge of the disc is pushed out and the torque acting on the disc is smaller, or an abnormally thick disc, which is unlikely. We have also shown that the density and temperature profiles of the disc can play a significant role in the magnitude of the disc warping and the inclination damping timescale, with more strongly 'flaring' discs (i.e. discs with rapidly growing scaleheight H) allowing the inclination to survive for a larger fraction of the disc's lifetime.

Applying our analytical results to circumstellar discs in binaries, we find that inclined discs tend to have very small warps (and smaller than circumbinary discs). Our results are, in this respect, significantly more favorable for the survival of large inclinations in circumstellar discs than previous studies which rely on the global properties of the disc to estimate this damping timescale. Thus, misaligned circumstellar discs are expected to be quite common in proto-binaries. Qualitatively, the key difference between circumbinary discs and circumstellar discs is that in former/latter, the binary torque is exerted at the inner/outer region of the disc, which contains small/larger amount of angular momentum, leading to relatively large/small warp and thus faster/slower viscous damping.

We have explored the possibility of efficient damping of disc warp through parametric instabilities associated with the strong velocity shears across the disc. Our updated estimate for the alignment timescale of the disc shows that, for circumbinary discs, the inclination angle above which parametric instabilities are likely to drive rapid damping of the inclination is small (about 4° for typical disc parameters; see Sec. 5.2), thus making it difficult to maintain inclination angles of more than a few degrees for a significant part of

the lifetime of the disc. The recent discoveries of circumbinary planetary systems with negligible or small inclinations (such as Kepler-413; see Kostov et al. 2014) between the binary plane and the planetary orbital plane are consistent with this picture. On the other hand, we find that significant misalignments could be possible in circumstellar discs, even when parametric instabilities are taken into account. In this respect, our predictions based on the approximate local prescription for the growth of parametric instabilities derived by Ogilvie & Latter (2013) differ from the earlier results of Bate et al. (2000), which predicted rapid damping of the inclination to less than the disc thickness H/r.

We have also showed that the above considerations apply not only to nearly aligned discs but also to relatively low mass (nearly) anti-aligned discs, except that in the latter case the disc may counter-align with the binary. The smaller inner radius of counter-aligned discs is also likely to make counter-alignment even faster than alignment.

As a concrete application of our model, we verified that our calculations are in agreement with the numerical results of Lodato & Facchini (2013), who modeled the precessing circumbinary disc system in KH 15D (following an earlier analytical model by Chiang & Murray-Clay 2004). Our result for the inclination damping shows that there exist some tensions between the required misalignment angle and the fact that that misalignment should be maintained for a few precession periods, at least if parametric instabilities damp the inclination efficiently. In that case, a misalignment angle of $\sim 10^\circ$ can only be maintained for ~ 10 precession periods, if the parameters of the system are tuned appropriately. This is however sufficient to explain current observations - and the tensions disappear if the parametric instabilities do not lead to efficient inclination damping.

ACKNOWLEDGMENTS

This work has been supported in part by the NSF grants AST-1008245, AST-1211061 and the NASA grants NNX12AF85G, NNX14AG94G. FF gratefully acknowledges support from the Vincent and Beatrice Tremaine postdoctoral fellowship, from the NSERC Canada, from the Canada Research Chairs Program, and from the Canadian Institute for Advanced Research.

REFERENCES

Armstrong, D.J., et al. 2014, arXiv:1404.5617
Artymowicz P., Lubow S. H., 1994, ApJ, 421, 651
Bate, M.R., et al. 2000, MNRAS, 317, 773
Bate, M.R., Bonnell, I.A., Bromm, V. 2003, MNRAS, 339, 577
Capelo, H. L., et al. 2012, ApJ, 757, L18
Chiang E.I., Murray-Clay R.A. 2004, ApJ, 607, 913
Davis, C.J., Mundt, R., Eisloffel, J. 1994, ApJ, 437, L58
Doyle, L.R., Carter, J.A., Fabrycky, D.C., Slawson, R.W., Howell, S.B., et al. 2011, Science, 333, 1602
Facchini S., Lodato G., Price D.J., 2013, MNRAS, 433, 2142
Facchini S., Ricci L., Lodato G., 2014, arXiv:1406.2708, accepted by MNRAS
Foucart, F., Lai,.D. 2011, MNRAS, 412, 2799
Foucart, F., Lai,.D. 2013, ApJ, 764, 106
Fragner, M.M, Nelson, R.P. , A&A, 511, 77
Hioki, J. et al. 2011, PASJ, 63, 543
Kennedy, G. M., et al. 2012a, MNRAS, 421, 2264
Kennedy, G. M., et al. 2012b, MNRAS, 426, 2115
King A.R., Lubow S.W., Ogilvie G.H., Pringle J.E., 2005, MNRAS, 363, 49
Klessen, R.S. 2011, EAS Pub. Series, 51, 133
Kostnov, V.B. et al. 2014, ApJ, 784, 14
Johnson J. A.,Marcy G.W., Hamilton C. M., et al. 2004, AJ, 128,1265
Larwood J.D, Papaloizou J.C.B., 1997, MNRAS, 285, 288
Lodatto G., Price D.J., 2010, MNRAS, 405, 1212
Lodatto G., Facchini S., 2013, MNRAS, 433, 2157
Lubow, S. H., Ogilvie G. I., 2000, ApJ, 538, 326
Lubow S. H., Ogilvie G. I. Pringle, J.E. 2002, MNRAS, 337, 706
Martin, D.V., Triaud, A.H.M.J. 2014, arXiv:1404.5360
Gammie C. F., Goodman J., Ogilvie G. I., 2000, MNRAS, 318, 1005
McKee C.F., Ostriker, E.C. 2007, ARAA, 45, 565
Ogilvie G.I., 1999, MNRAS, 304, 557
Ogilvie G.I., 2006, MNRAS, 365, 977
Ogilvie G.I., Latter H.N., 2013, MNRAS, 433, 2420
Orosz, J.A., et al. 2012, Science, 337, 1511
Papaloizou J.C.B., Lin D.N.C., 1995, ApJ, 438, 841
Papaloizou J.C.B., Pringle J.E., 1983, MNRAS, 202, 1181
Papaloizou J.C.B., Terquem C., 1995, MNRAS, 274, 987
Roccatagliata, V., Ratzka, T., Henning, T., Wolf, S., Leinert, C., & Bouwman, J. 2011, A&A, 534, A33
Sorathia K. A., Krolik J. H., Hawley J. F., 2013a, ApJ, 768, 133
Sorathia K. A., Krolik J. H., Hawley J. F., 2013b, ApJ, 777, 21
Stapelfeldt, K.R., et al. 1998, ApJ, 502, L65
Teixeira, D.M., Fragile, P.C., Zhuravlev, V.V., Ivanov, P.B., 2014, arXiv:1406.5514
Welsh, W.F., Orosz, J.A., Carter, J.A., Fabrycky, D.C., Ford, E.B., et al. 2012 Nature, 481, 475
Williams, J.P., Cieza, L.A. 2011, ARAA, 49, 67
Winn J. N., Holman M. J., Johnson J. A., et al. 2004, ApJ, 603, L45

APPENDIX A: SHAPE FUNCTIONS FOR POWER-LAW DISC PROFILES

In the case of a power-law disc profile,

$$\Sigma(r) = \Sigma_{\rm in}\left(\frac{r}{r_{\rm in}}\right)^{-p}, c_s(r) = c_{\rm in}\left(\frac{r}{r_{\rm in}}\right)^{-c}, \tag{A1}$$

$$Z(r) = Z_{\rm in}\left(\frac{r}{r_{\rm in}}\right)^{-z}, K(r) = K_{\rm in}\left(\frac{r}{r_{\rm in}}\right)^{-k}, \tag{A2}$$

$$\Omega(r) = \Omega_{\rm in}\left(\frac{r}{r_{\rm in}}\right)^{-3/2}. \tag{A3}$$

the shape functions Γ defined in Sec. 2.2 can be written analytically.

$$\Gamma_p = \frac{F(1,x_{\rm out};1-p-z)}{F(1,x_{\rm out};5/2-p)} \quad \text{(A4)}$$

$$\Gamma_G(x) = F(1,x;1-p-z) - \Gamma_p F(1,x;5/2-p) \quad \text{(A5)}$$

$$\Gamma_1(x) = \Gamma_p \int_x^{x_{\rm out}} dy\, y^{p+2c-3/2}\Gamma_G(y) \quad \text{(A6)}$$

$$\Gamma_2(x) = \int_x^{x_{\rm out}} dy\, y^{p+2c-k-3}\Gamma_G(y) \quad \text{(A7)}$$

$$\Gamma_3(x) = \int_x^{x_{\rm out}} dy\, y^{p+2c-3}\Gamma_G(y) \quad \text{(A8)}$$

$$\Gamma_I = \frac{\int_1^{x_{\rm out}} dy\, y^{p+2c-3}\Gamma_G^2(y)}{F(1,x_{\rm out};5/2-p)} \quad \text{(A9)}$$

$$= \frac{\int_1^{x_{\rm out}} dy \left(y^{-p-z} - \Gamma_p y^{3/2-p}\right)\Gamma_3(y)}{F(1,x_{\rm out};5/2-p)} \quad \text{(A10)}$$

where we defined $F(x,y;n)$ as

$$F(x,y;a) = \frac{y^a - x^a}{a}\,(a\neq 0) \quad \text{(A11)}$$

$$= \ln(y/x)\,(a=0) \quad \text{(A12)}$$

From these equations, we can clearly see that $\Gamma_G(1) = \Gamma_G(x_{\rm out}) = 0$, and thus $\boldsymbol{G}$ respects the no-torque boundary condition. The integral expressions for $\Gamma_{1,2,3}$ are easy to compute, but relatively cumbersome. Under the relatively general assumption that $p < 5/2$ and $p+z > 1$, we get

$$\Gamma_1(x) = -\Gamma_p^2\frac{F(x,x_{\rm out};2+2c) - F(x,x_{\rm out};p+2c-1/2)}{5/2-p} + \Gamma_p\frac{F(x,x_{\rm out};2c-z+1/2) - F(x,x_{\rm out};p+2c-1/2)}{1-p-z}$$

$$\Gamma_2(x) = -\Gamma_p\frac{F(x,x_{\rm out};1/2+2c-k) - F(x,x_{\rm out};p+2c-2-k)}{5/2-p} + \frac{F(x,x_{\rm out};2c-z-1-k) - F(x,x_{\rm out};p+2c-2-k)}{1-p-z}$$

$$\Gamma_3(x) = -\Gamma_p\frac{F(x,x_{\rm out};1/2+2c) - F(x,x_{\rm out};p+2c-2)}{5/2-p} + \frac{F(x,x_{\rm out};2c-z-1) - F(x,x_{\rm out};p+2c-2)}{1-p-z}.$$

Finally, Γ_I can be recovered using the identity

$$\int_1^{x_{\rm out}} dy\, y^{a-1}F(y,x_{\rm out};b) = \frac{F(1,x_{\rm out};a+b) - F(1,x_{\rm out};b)}{a} \quad \text{(A13)}$$

which is valid for $a \neq 0$. We then get

$$\Gamma_I = \frac{1}{F(1,x_{\rm out};5/2-p)}\left(\frac{\Gamma_p\Gamma_3(1;0)}{5/2-p} - \frac{\Gamma_3(1;0)}{1-p-z} + \frac{\Gamma_3(1;1-p-z)}{1-p-z} - \frac{\Gamma_p\Gamma_3(1;5/2-p)}{5/2-p}\right) \quad \text{(A14)}$$

with the notation

$$\Gamma_3(x;A) = -\Gamma_p\frac{F(x,x_{\rm out};1/2+2c+A) - F(x,x_{\rm out};p+2c-2+A)}{5/2-p} + \frac{F(x,x_{\rm out};2c-z-1+A) - F(x,x_{\rm out};p+2c-2+A)}{1-p-z}.$$